

# **Chapter 3. Gas Phase Reactions of Methyl Phosphate in Clusters and the Effect of Sodium Ions on Dissociation Pathways**

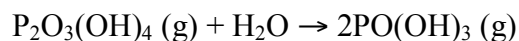
## **3.1. Introduction**

Phosphate ions are ubiquitous in biological systems. The major energy storage molecule of living systems is adenosine triphosphate (ATP), and deoxyribonucleic acid, the genetic code, is linked together with a phosphate backbone. Organogenic phosphate has been found in the oldest preserved sedimentary records, indicating its vital importance to the origins of life.<sup>1</sup> This involvement with the origin of life is ascribed to phosphate's unique properties, including its reactivity.<sup>2</sup> Polyphosphate can serve as a substitute for ATP in some organisms,<sup>3</sup> and may have been the original energy source in prebiotic evolution.<sup>4</sup> However, the mechanism by which phosphate ions were condensed to form meta- and polyphosphates is unclear.<sup>5</sup> It has been suggested that volcanic activity was responsible for polyphosphate formation,<sup>6</sup> or that high-energy organic compounds could be responsible for polyphosphate formation,<sup>7</sup> but the ability of these reaction pathways to account for prebiotic polyphosphate synthesis is not firmly established.<sup>8</sup> Thus, it is of interest to study the formation of polyphosphates and examine the factors that facilitate or inhibit their creation.

Hydrolysis of ATP in solution under biochemical standard conditions,



has a standard Gibbs free energy  $\Delta G^\circ = -30.5 \text{ kJ/mol}$ ,<sup>9</sup> and the phosphorus-oxygen bond in polyphosphates is often described as a high-energy bond. However, density functional theory calculations on gas phase hydrolysis of diphosphate



gives a hydrolysis enthalpy of +3 kJ/mol, or a near-zero enthalpy change.<sup>10</sup> This should be comparable to the Gibbs free energy change in solution, as the entropy contribution to is probably fairly small. Julian and Beauchamp suggest that gas phase reactions in salt clusters may have played a role in the prebiotic synthesis of ATP.<sup>11</sup> The increased stability of polyphosphates in the gas phase as compared with solution phase would tend to support this viewpoint.

Polyphosphate ions have also proven to be of interest in the study of cluster phase reactions that occur between non-covalently bound species in the gas phase.<sup>11-13</sup> While energetic activation of non-covalently bound clusters in the gas phase often leads to dissociation, under certain conditions, intermolecular reactions can occur. Some design criteria leading to reactive clusters have been previously outlined.<sup>13</sup> In clusters meeting these criteria, triphosphate has been observed to phosphorylate peptides selectively at hydroxyl residues.<sup>12</sup> Collisional activation of trimers of AMP has resulted in a gas phase synthesis of ATP. This reaction is dependent on having AMP present as a sodium salt, with the addition or loss of a sodium ion yielding, respectively, the reactive cationic and anionic clusters.<sup>11</sup> Clusters containing no sodium ions dissociate rather than react, indicating that the sodium cations provide additional binding energy to the cluster and allows the formation and cleavage of covalent bonds to compete with dissociation.

However, the anionic phosphate dimer,  $[(\text{H}_3\text{PO}_4)_2 - \text{H}]^-$ , reacts to lose water and form a diphosphate anion.<sup>14</sup> In this system, no sodium is required for reaction to occur.

To further understand the details of phosphate bond formation and the relationship of cluster reactivity to the presence or absence of sodium ions, a systematic study was conducted on negatively charged clusters of methyl phosphate containing varying numbers of sodium cations,  $[(\text{MeH}_2\text{PO}_4)_n - (x + 1)\text{H} + x \text{Na}]^-$ , where  $0 \leq x \leq n - 1$ . We find that reactivity is highly dependent on cluster size, as well as on the number of sodium ions contained in a cluster. For small clusters,  $n = 2$ , a phosphate bond can be formed in the absence of sodium. Clusters of  $n = 3$  to  $n = 5$  follow the pattern observed for AMP, as only the sodium salt clusters evince high levels of phosphate bond formation. However, as clusters grow in size ( $n > 5$ ), sodium salt clusters no longer possess sufficient binding energy to keep simple cluster dissociation from competing with more complex reactions.

## 3.2. Experimental

All experiments were performed on a Finnigan LCQ Deca ion trap mass spectrometer with an ESI source operating in the negative ion mode. Ions were subjected to collisional activation for 30 ms. Relative product yields were measured as relative peak intensities in the mass spectrum. There may be small systematic variation in detection sensitivity at different masses, but this was not investigated.

Samples were electrosprayed from methanol solutions and contained methyl phosphate at a concentration of 100  $\mu\text{M}$ , and alkali ion hydroxide salts at concentrations of 30 to 50  $\mu\text{M}$ . Solution flow rates were between 3 and 5  $\mu\text{L}/\text{min}$ . All compounds were purchased from Sigma-Aldrich and used without further purification. Experiments on

negative ion adducts were repeated on a Finnigan LCQ Classic mass spectrometer and were found to be highly reproducible.

### 3.3. Results and Discussion

The negative ion ESI-MS spectrum of an electrosprayed solution of methyl phosphate, with sodium chloride added, is shown in Figure 3.1. The major peak in the spectrum corresponds to singly deprotonated methyl phosphate,  $\text{MeHPO}_4^-$ . Distinct patterns of clusters are evident in the spectrum. The largest cluster observed with high enough abundance for CID experiments is composed of seven methyl phosphates and six sodium ions. Some representative clusters are labeled in Figure 3.1. The addition of sodium chloride to the solution causes clusters with sodium ions to be present in greater abundance than the non-sodiated species.

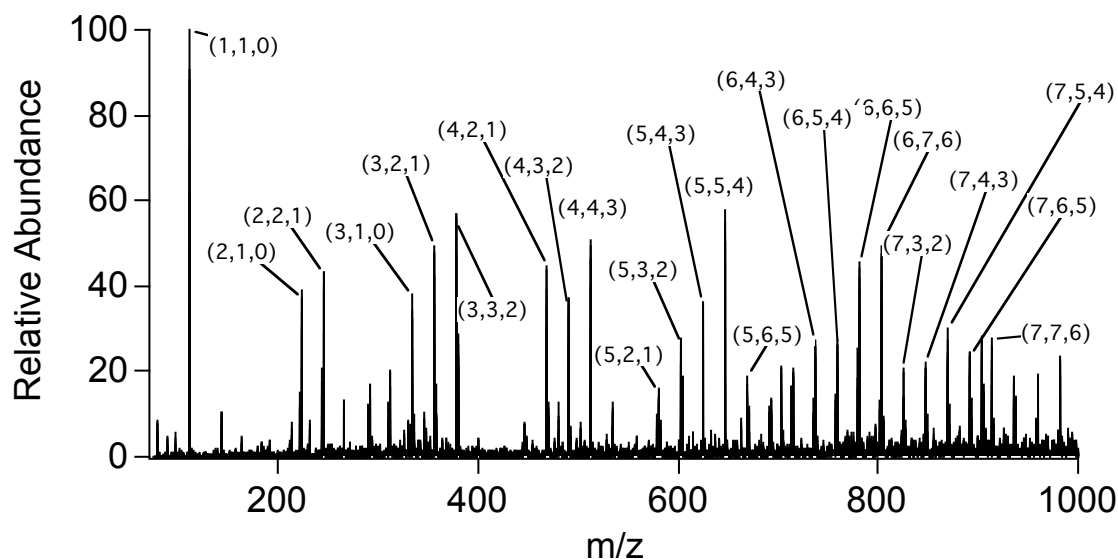


**Figure 3.1.** Full mass spectrum of 100  $\mu\text{M}$  methyl phosphate and 30  $\mu\text{M}$  NaCl. The peaks are marked as  $(h,k,l)$ , which indicates the species  $[(\text{MeH}_2\text{PO}_4)_h - k\text{H} + l\text{Na}]^-$ .

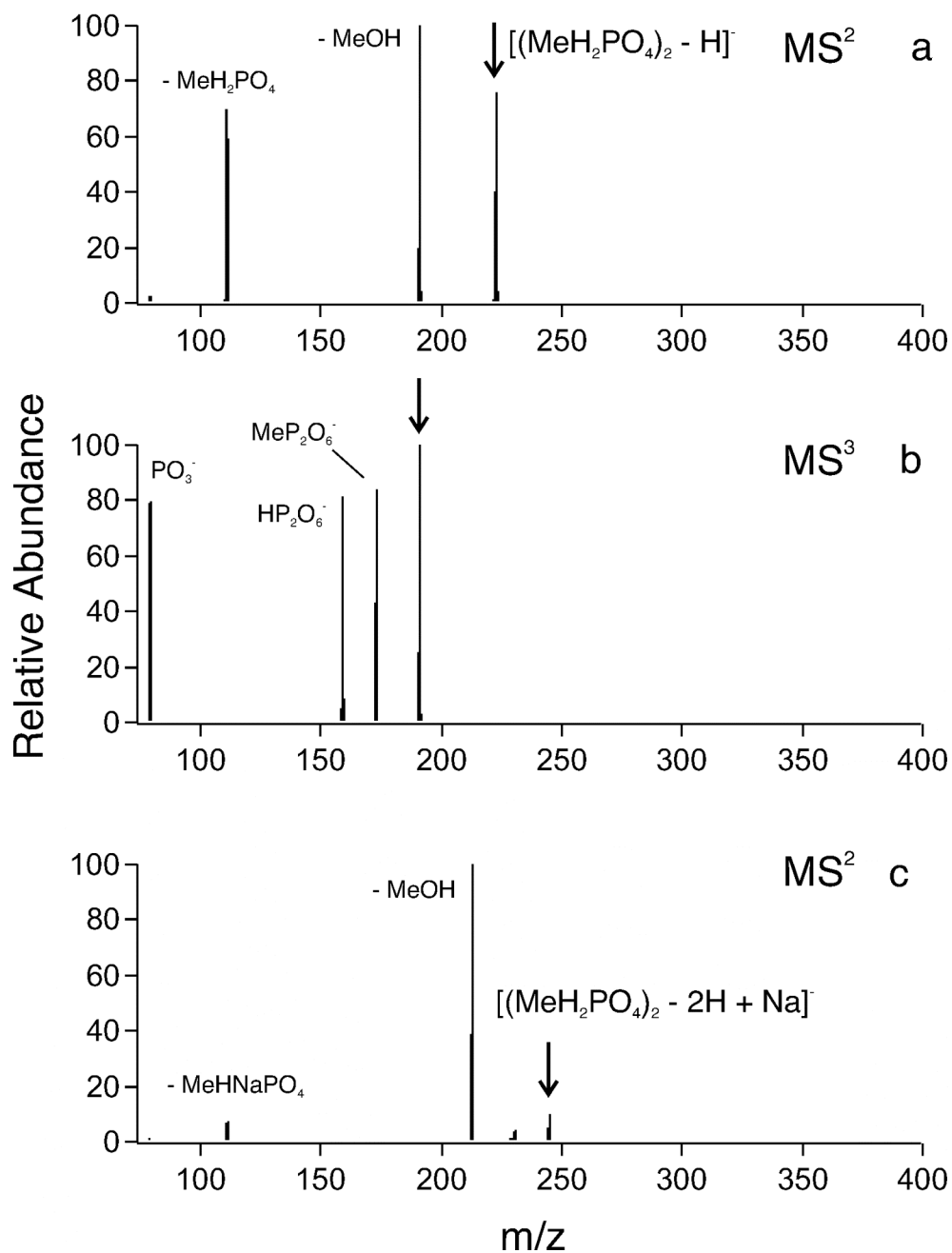
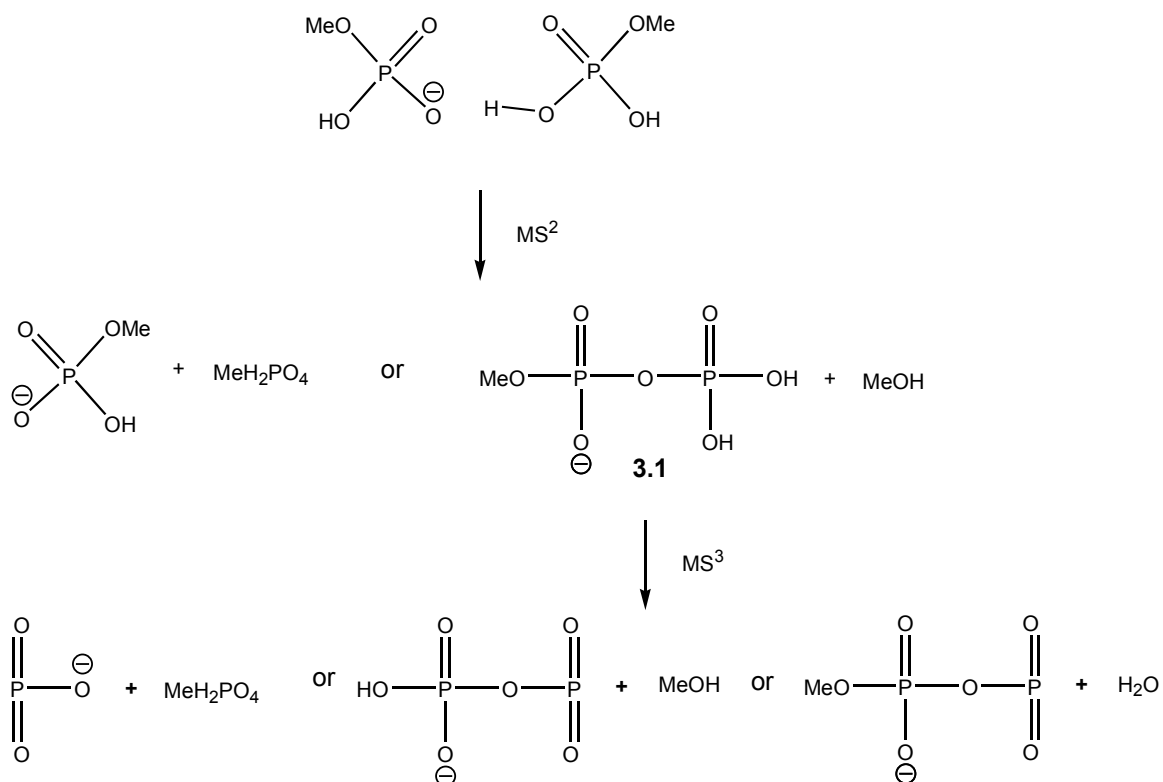


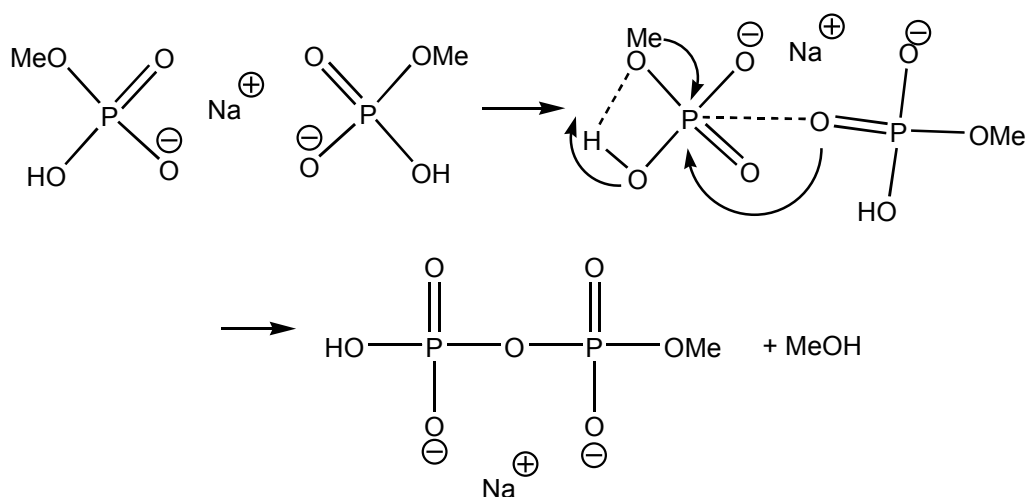
**Figure 3.2.** (a) CID spectrum of  $[(\text{MeH}_2\text{PO}_4)_2 - \text{H}]^-$ . A loss of methanol (190.9 m/z) is observed, as is the dissociation of the methyl phosphate dimer (110.9 m/z). (b) MS<sup>3</sup> spectrum showing the loss of methanol and water, as well as MeH<sub>2</sub>PO<sub>4</sub>, from the peak at 190.9 m/z in (a). (c) CID spectrum of  $[(\text{MeH}_2\text{PO}_4)_2 - 2\text{H} + \text{Na}]^-$ . Note the increased loss of methanol compared to the spectrum shown in (a).

Isolation of the negatively charged methyl phosphate dimer,  $[(\text{MeH}_2\text{PO}_4)_2 - \text{H}]^-$ , leads to two products, as shown in Figure 3.2a. The dominant product is the loss of methanol, which would result from proton transfer from a hydroxyl group to the methoxy group. Dissociation of  $\text{MeH}_2\text{PO}_4$  from the cluster, resulting in  $\text{MeHPO}_4^-$ , is also observed. Previous work has shown that clusters of  $[n\text{AMP} - n\text{H} + (n - 1)\text{Na}]^-$  will react to form ADP under CID, and that phosphoric acid reacts under CID to form diphosphate,<sup>11</sup> in analogous reactions. Figure 3.2b shows the CID spectrum of **3.1**, found at 190.9 m/z. The major products are  $\text{MeP}_2\text{O}_6^-$  (loss of water),  $\text{HP}_2\text{O}_6^-$  (loss of methanol), and  $\text{PO}_3^-$  (loss of methyl phosphate), shown in Scheme 3.1. These losses are consistent with the assignment of this peak to methyl diphosphate. It is reasonably certain that this system is reacting in the same way as other phosphate clusters and forming a new phosphorus-oxygen bond, as shown in Scheme 3.1.



**Scheme 3.1.** Reaction products from  $\text{MS}^2$  and  $\text{MS}^3$  of  $[(\text{MeH}_2\text{PO}_4)_2 - \text{H}]^-$ .

The condensation product **3.1** can be formed via an associative mechanism, as proposed by both Williams<sup>14</sup> and Beauchamp<sup>11</sup> and shown in Scheme 3.2. This involves a pentacoordinate phosphorus intermediate. In the gas phase, the hydrolysis is thought to take place in a concerted reaction, in which proton transfer to the methoxy group occurs at the same time as P-O bond cleavage, while in solution, a zwitterionic intermediate,  $\text{CH}_3\text{O}^+(\text{H})\text{PO}_3^{2-}$ , is formed.<sup>15-17</sup> The presence of a counterion has been found to stabilize the gas phase zwitterionic intermediate by bridging the two oxygen atoms of the metaphosphate fragment.<sup>16</sup>



**Scheme 3.2. Associative reaction of two methyl phosphates bound by sodium.**

Figure 3.2c shows the CID spectrum obtained when the cluster  $[(\text{MeH}_2\text{PO}_4)_2 - 2\text{H} + \text{Na}]^-$  is dissociated. Most of the product observed is due to methanol loss, although a small amount of  $\text{MeHPO}_4^-$  (< 10% of the most intense ion) is also observed. While the sodium ion is not required for formation of methyl diphosphate, the presence of the sodium ion increases the efficiency of the intermolecular reaction relative to the efficiency of dissociation. This is in contrast to the observed behavior of AMP and phosphoric acid clusters, which dissociated easily when no sodium ion was present.<sup>11</sup>



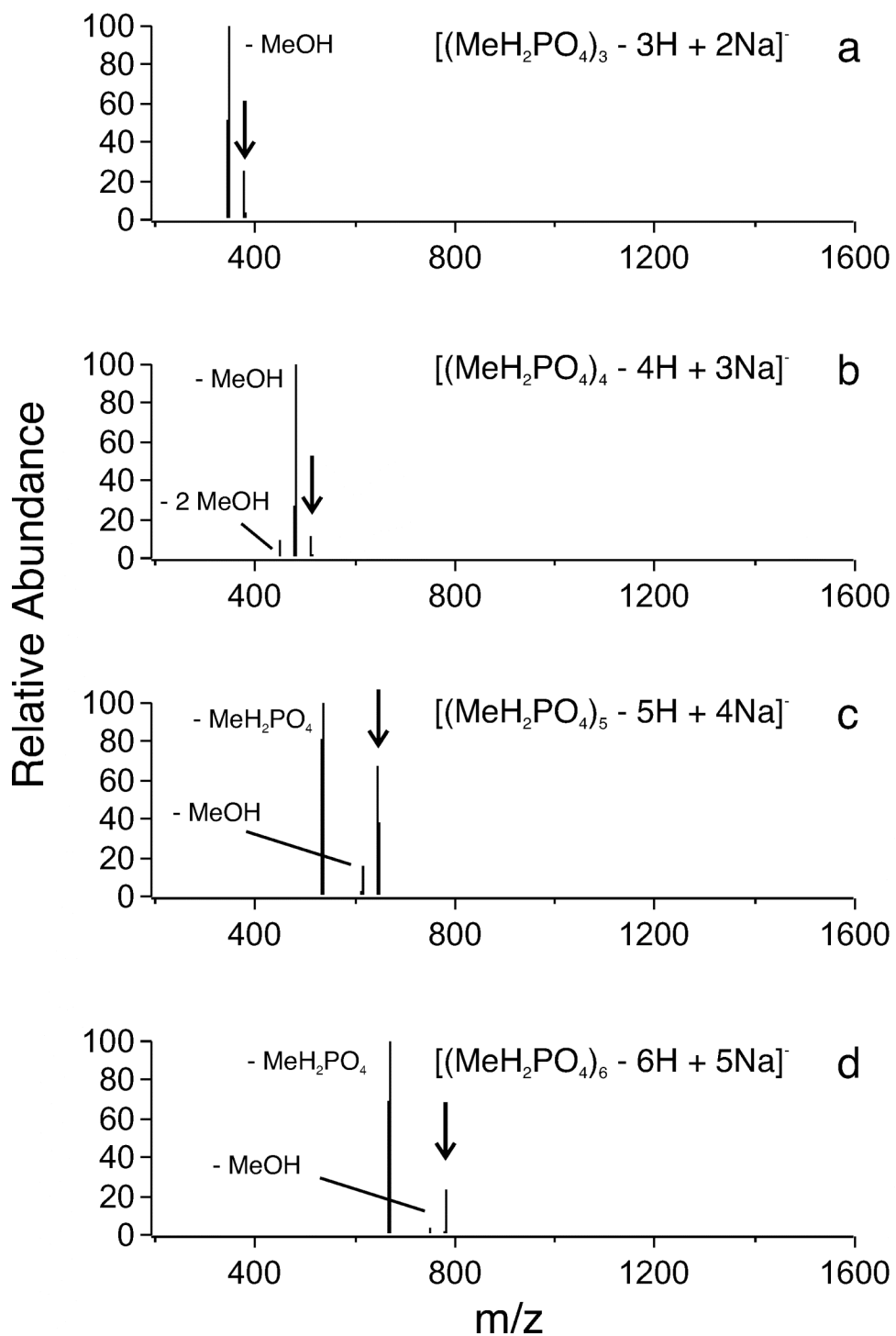


**Figure 3.3.** Collision-induced dissociation of (a)  $[(\text{MeH}_2\text{PO}_4)_3 - 3\text{H} + 2\text{Na}]^-$ , (b)  $[(\text{MeH}_2\text{PO}_4)_4 - 4\text{H} + 3\text{Na}]^-$ , (c)  $[(\text{MeH}_2\text{PO}_4)_5 - 5\text{H} + 4\text{Na}]^-$ , (d)  $[(\text{MeH}_2\text{PO}_4)_6 - 6\text{H} + 5\text{Na}]^-$ . As the cluster grows larger, the loss of  $\text{MeH}_2\text{PO}_4$  becomes more probable.

In general, negatively charged clusters  $[(\text{MeH}_2\text{PO}_4)_n - (x + 1)\text{H} + x \text{Na}]^-$ , where  $0 \leq x \leq n - 1$ , were found to undergo one of two reactions, resulting in either a loss of neutral monomethyl phosphate (mass 112 Da) or a loss of methanol (mass 32 Da). In other words, either dissociation of the cluster components was observed, or a new phosphorus-oxygen bond was formed, as in Scheme 3.1. Figure 3.3 shows the results of CID on a series of negatively charged clusters,  $[(\text{MeH}_2\text{PO}_4)_x - (x + 1)\text{H} + x \text{Na}]^-$ , where  $x = 3 - 6$ . These can be referred to as salt clusters, as in each case the methyl phosphates in the cluster are deprotonated and coupled with a sodium cation (excepting the methyl phosphate carrying a negative charge). For  $x = 3$  and  $x = 4$ , the clusters undergo intermolecular condensation reactions and lose methanol almost exclusively. However, for larger clusters, the situation changes. Figure 3.3c shows the results of CID for  $x = 5$ . The most abundant product in this spectrum is from the loss of  $\text{MeH}_2\text{PO}_4$ , resulting from dissociation of the cluster components. A peak corresponding to loss of methanol is also present, but it is approximately five times lower in intensity. As the cluster size continues to increase, as shown in Figure 3.3d for  $x = 6$ , loss of  $\text{MeH}_2\text{PO}_4$  dominates the spectrum, which shows a very small peak corresponding to methanol loss. The data for  $x = 7$  (not shown) are very similar to the results obtained for  $x = 6$ . As size increases, it becomes more energetically favorable for the cluster to dissociate rather than react. The cluster  $[(\text{MeH}_2\text{PO}_4)_6 - 7\text{H} + 6\text{Na}]^-$  (not shown) shows a more significant loss of methanol than does the  $[(\text{MeH}_2\text{PO}_4)_6 - 6\text{H} + 5\text{Na}]^-$  cluster, indicating that a higher percentage of sodium in the cluster can compensate for the increase in cluster size and facilitate intermolecular reactions.

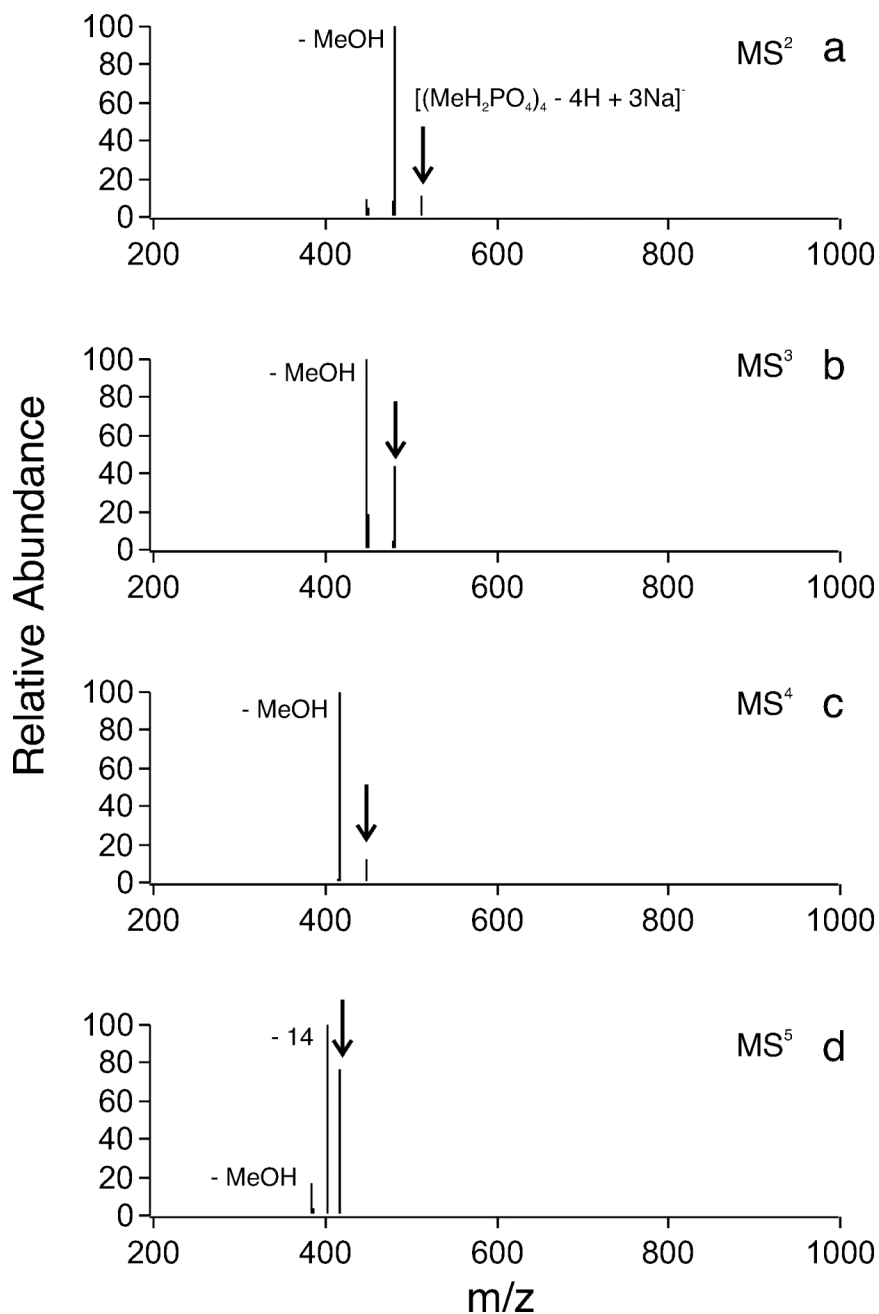
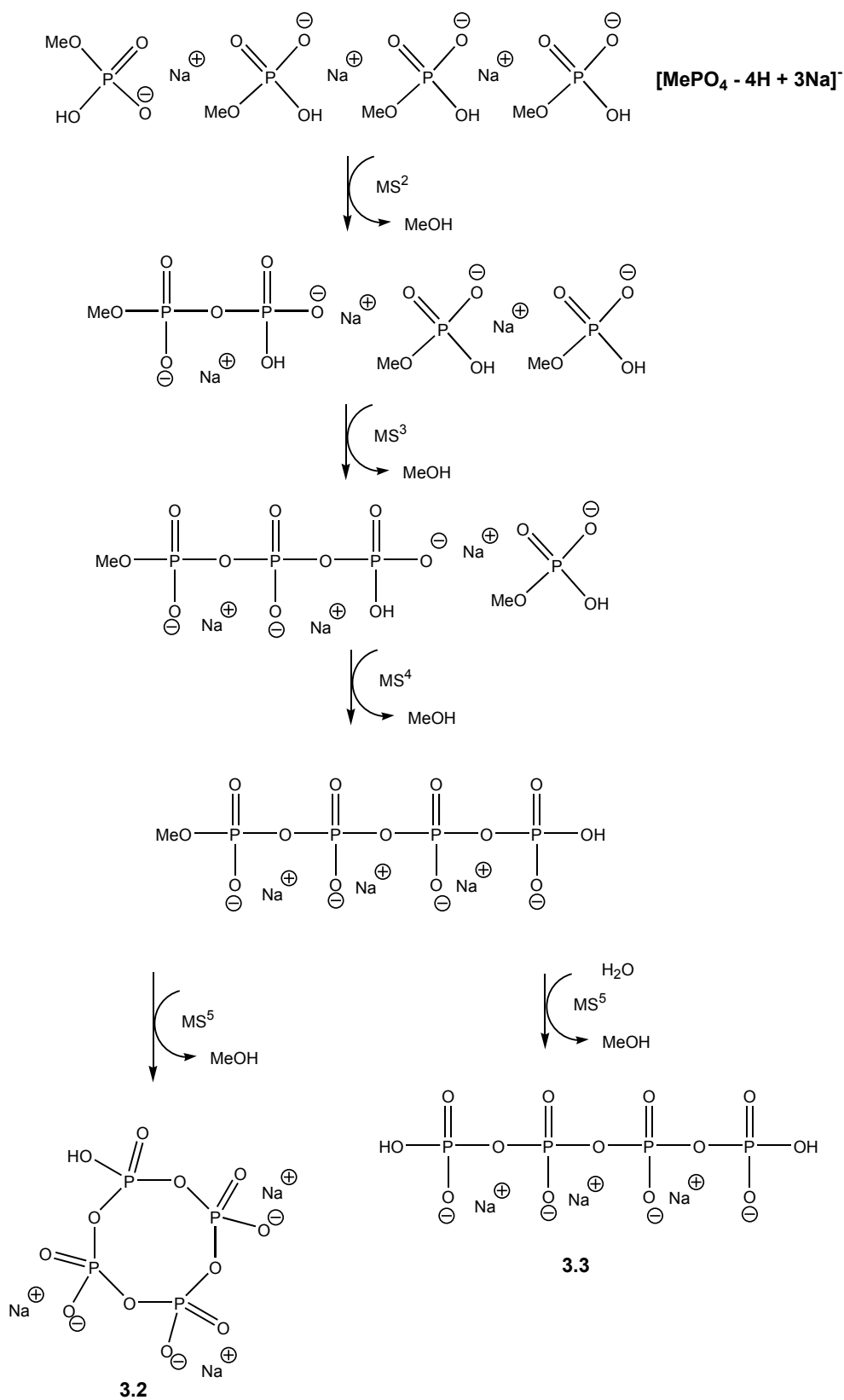


**Figure 3.4.** (a) MS<sup>2</sup> of the cluster  $[(\text{MeH}_2\text{PO}_4)_4 - 4\text{H} + 3\text{Na}]^-$ . The largest product peak corresponds to loss of methanol. (b) Methanol is lost again, resulting in a triphosphate ion. (c) A third methanol loss is observed to form methyl tetraphosphate. (d) MS<sup>5</sup> on the condensed product shows loss of 14 Da as the most abundant product peak and a small loss of methanol.

In several cases, the product resulting from loss of methanol was dissociated sequentially. Typical results from this procedure are shown in Figure 3.4 for  $[(\text{MeH}_2\text{PO}_4)_4 - 4\text{H} + 3\text{Na}]^-$ . Methanol is lost sequentially three times, resulting in the formation of negatively charged trisodium methyl tetraphosphate. In the last dissociation step, shown in Figure 3.4d, a loss of 14 Da is observed most prominently, with a small loss of methanol (32 Da) also observed. Scheme 3.3 shows the sequence of reactions that produce the spectra shown in Figure 3.4. Three sequential activation steps result in sequential losses of methanol from the cluster, finally resulting in the formation of a tetraphosphate species. This species can either react intramolecularly, to form a cyclic pyrophosphate such as **3.2**, or it can pick up water in the trap and lose methanol to form negatively charged trisodium tetraphosphate (**3.3**).

The breakup of sodium diphosphate resulting from  $\text{MS}^3$  of the  $[(\text{MeH}_2\text{PO}_4)_2 - 2\text{H} + \text{Na}]^-$  cluster shows loss of  $\text{NaMeHPO}_4$  (the major product) and loss of methanol (a minor product). The fully condensed sodium triphosphate species resulting from sequential CID on the  $[(\text{MeH}_2\text{PO}_4)_3 - 3\text{H} + 2\text{Na}]^-$  cluster, when broken up, also loses methanol and  $\text{NaMeHPO}_4$ , but the most prominent loss observed is that of 14 Da. As the size of the cluster increases, the fully condensed product is more likely to pick up a water molecule and lose methanol than to undergo an intramolecular reaction.



**Scheme 3.3.** Reactions observed for the  $[(\text{MeH}_2\text{PO}_4)_4 - 4\text{H} + 3\text{Na}]^-$  cluster.

The fully condensed product clusters are less likely to undergo intramolecular reactions as the initial cluster size grows larger. Clusters containing more methyl phosphates should be more likely to exhibit condensed phase behavior. Therefore, it is of interest to compare the larger clusters with sodium metaphosphate glass, a condensed phase structure formed by heating  $\text{NaH}_2\text{PO}_4 \cdot 2\text{H}_2\text{O}$  over a desiccant.<sup>18</sup> The resulting glass has the empirical formula  $\text{NaPO}_3$ . X-ray diffraction studies have determined that the close-order structure of sodium metaphosphate glass, shown in Figure 3.5a, consists of a  $\text{PO}_4$  tetrahedron, with two corners coordinated to sodium ions (which coordinate to other  $\text{PO}_4$  tetrahedra) and two corners coordinated to different  $\text{PO}_4$  tetrahedra. The sodium ions facilitate formation of a linear structure in the sodium metaphosphate glass.

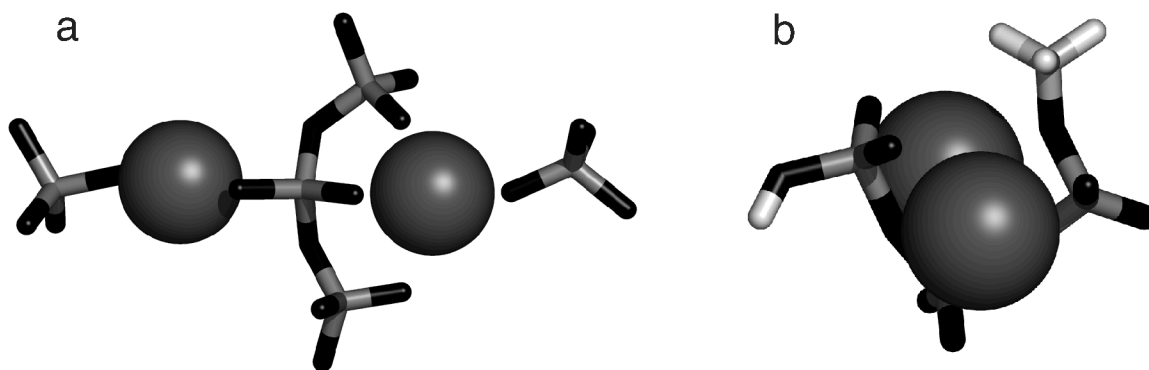


**Figure 3.5. (a) Close-order structure of sodium metaphosphate glass determined by X-ray diffraction.<sup>18</sup> (b) Structure of fully condensed, singly negatively charged methyl triphosphate with two sodium ions from PM5 calculations. Sodiums are shown in space-filling representations for clarity.**

Figure 3.5b shows a theoretical structure of the fully condensed ( $\text{MS}^3$ ), singly negatively charged methyl triphosphate formed from sequential collisional activations of the  $[(\text{MeH}_2\text{PO}_4)_3 - 3\text{H} + 2\text{Na}]^-$  cluster. As in the crystal structure of sodium

metaphosphate glass, a central  $\text{PO}_4$  group is attached to two sodium ions and two  $\text{PO}_4$  tetrahedra. The sodium ions do not continue in the linear network found in the condensed phase, but move inward to coordinate with oxygen atoms on the peripheral phosphate groups, thus increasing charge stabilization within the cluster. (The structure shown in Figure 3.5b, with the proton and the methyl group on different phosphate units, is more stable by 20 kJ/mol than the structure in which both the proton and methyl group are located on one phosphate unit.)

The lack of intramolecular reactivity in the fully condensed cluster, such as that shown in Figure 3.5b, may be attributed to the structure of the cluster. The proton is not well-positioned to interact with the methoxy group and undergo intramolecular reaction. Because of the diminished reactivity of the fully condensed species for large polyphosphates, the molecule is more likely to pick up a water molecule before dissociation. Water catalyzes the reaction by providing a proton for the methoxy group to abstract, resulting in formation of a species such as **3.3**.

### **3.4. Conclusion**

Phosphate has proven to be an extremely versatile functional group useful in the design of cluster phase reactions.<sup>11-13</sup> In solution, this unique reactivity makes phosphate the energy source for life; in the gas phase, this allows for exploration of reactions between non-covalently bound species via collision-induced dissociation. It has been previously noted<sup>11</sup> that sodiation of a cluster of AMP or phosphoric acid favors reaction rather than dissociation of cluster components. In particular, when each AMP present in a cluster was deprotonated and coupled with a sodium cation, in a salt cluster, reactions to produce diphosphate were observed. The results presented here for methyl phosphate

indicate that for small clusters with two methyl phosphate ions, reaction between phosphorus and oxygen occurs even when no sodium ions are present in a cluster. This phenomenon has also been observed with the phosphate dimer,  $[(\text{H}_3\text{PO}_4)_2 - \text{H}]^-$ , which loses  $\text{H}_2\text{O}$  to form a pyrophosphate ion.<sup>14</sup>

Additionally, for larger cluster sizes (more than five methyl phosphate ions), salt clusters no longer provide enough enhanced binding energy to prevent dissociation of neutral methyl phosphate and facilitate phosphorus-oxygen bond formation. As the cluster size increases, higher percentages of sodium ions are necessary to favor phosphorus-oxygen bond formation. The binding energy of each successive  $\text{NaMeHPO}_4$  unit to a core of  $(\text{NaMeHPO}_4)_n\text{MeHPO}_4^-$  is weaker than the last, until, at large values of  $n$ , the binding energy of the cluster is less than the activation barrier for reaction. This may impose a natural limit on the size of biopolymers that can be fabricated in the gas phase using this technique.

The structure of the larger methyl polyphosphate-sodium clusters may resemble the structure of the condensed phase sodium phosphate glass. Other cluster studies on alkali-halide salts,<sup>19</sup> transition-metal nitrides,<sup>20</sup> and alkali-earth metal oxide clusters<sup>21,22</sup> have revealed clusters of extra stability corresponding to microcrystalline particles in the gas phase. Large condensation products of multiple collisional activations, such as negatively charged trisodium tetrphosphate, are large enough to react intramolecularly fairly easily. However, the negatively charged trisodium methyl tetrphosphate formed in the experiment shown in Figure 3.4 is far more likely to pick up water from the trap and undergo an intermolecular reaction to become negatively charged trisodium tetrphosphate than to undergo an intramolecular reaction. This can be explained if the



condensation product adopts the stable configuration shown in Figure 3.5b, which resembles that of condensed phase sodium metaphosphate glass.

### 3.5. References

- (1) Arrhenius, G.; Sales, B.; Mojzsis, S.; Lee, T. *J. Theor. Biol.* **1997**, *187*, 503.
- (2) Westheimer, F. H. *Science* **1987**, *235*, 1173.
- (3) Wood, H. G. *Curr. Top. Cell. Regul.* **1985**, *26*, 355.
- (4) Kornberg, A.; Rao, N. N.; Ault-Riché, D. *Annu. Rev. Biochem.* **1999**, *68*, 89.
- (5) Chyba, C. F.; McDonald, G. D. *Annu. Rev. Earth Planet. Sci.* **1995**, *23*, 215.
- (6) Yamagata, Y.; Watanabe, H.; Saitoh, M.; Namba, T. *Nature* **1991**, *352*, 516.
- (7) Miller, S. L.; Parris, M. *Nature* **1964**, *204*, 1248.
- (8) Keefe, A. D.; Miller, S. L. *J. Mol. Evol.* **1995**, *41*, 693.
- (9) Lehninger, A. L.; Nelson, D. L.; Cox, M. M. *Principles of Biochemistry*, 2nd ed.; Worth Publishers: New York, 1993.
- (10) Johnson, J. R. T.; Panas, I. *Chem. Phys. Lett.* **2001**, *348*, 433.
- (11) Julian, R. R.; Beauchamp, J. L. *Int. J. Mass Spectrom.* **2003**, *227*, 147.
- (12) Cox, H. A.; Hodyss, R.; Beauchamp, J. L. *J. Am. Chem. Soc.* **2005**, *127*, 4084.
- (13) Hodyss, R.; Cox, H. A.; Beauchamp, J. L. *J. Phys. Chem. A* **2004**, *108*, 10030.

- (14) Strittmatter, E. F.; Schnier, P. D.; Klassen, J. S.; Williams, E. R. *J. Am. Soc. Mass Spectrom.* **1999**, *10*, 1095.
- (15) Hu, C.-H.; Brinck, T. *J. Phys. Chem. A* **1999**, *103*, 5379.
- (16) Bianciotto, M.; Barthelat, J.-C.; Vigroux, A. *J. Phys. Chem. A* **2002**, *106*, 6521.
- (17) Bianciotto, M.; Barthelat, J.-C.; Vigroux, A. *J. Am. Chem. Soc.* **2002**, *124*, 7573.
- (18) Brady, G. W. *J. Chem. Phys.* **1958**, *28*, 48.
- (19) Beck, R. D.; St. John, P.; Homer, M. L.; Whetten, R. L. *Science* **1991**, *253*, 879.
- (20) Chen, Z. Y.; Castleman, A. W., Jr. *J. Chem. Phys.* **1993**, *98*, 231.
- (21) Ziemann, P. J.; Castleman, A. W., Jr. *J. Chem. Phys.* **1991**, *94*, 718.
- (22) Ziemann, P. J.; Castleman, A. W., Jr. *J. Phys. Chem.* **1992**, *96*, 4271.